LROC NAC SOUTH POLE CONTROLLED MOSAIC. R. V. Wagner, A. K. Boyd, M. R. Henriksen, M. R. Manheim, E. J. Speyerer, and M. S. Robinson. School of Earth and Space Exploration, Arizona State University, Tempe, AZ 85287-3603 (rvwagner@asu.edu).

Introduction: With the increased interest in the south polar region of the Moon from the Artemis program, CLPS missions, and international missions, there is a clear need for high-resolution controlled mosaics of the region. Our goal is to align most or all Lunar Reconnaissance Orbiter Camera (LROC) Narrow Angle Camera (NAC) images of the south polar region (poleward of 84° S) to within ~5 m of their true position.

Due to the evolution of the LRO orbit obliquity the NACs can now only acquire nadir images equatorward of 85° latitude. This is thus a good time finalize control of this key dataset. Additionally, we can take advantage of recent improvements to the polar Lunar Orbiter Laser Altimeter (LOLA) tracks and LOLA-controlled terrain models near the south pole for absolute control **[1]**.

We determined that the existing uncontrolled south polar images have offsets up to ~100 m from their true positions (worse than anticipated from equatorial images), which is not suitable for detailed geologic mapping and mission planning. Our prior attempts at using the ISIS bundle-block adjustment routine *jigsaw* **[2]** on polar images did not produce well-controlled results and could not extend to the entire polar dataset with available resources. In this effort, we adopted a brute-force automated control method to align images in 2D map space. We expect to get slightly worse results than a perfect bundle adjustment, as the correction is done after map-projection onto the 3D lunar shapemodel, which will cause some distortion. However, this method should be a major improvement on uncontrolled images, with good image-to-image registration across all lighting conditions.

Basic assumptions: Our primary assumption is that the map-projected images are correctly positioned on the surface (to ±~100 m), correctly oriented, and correctly scaled. That is, a projected image can be accurately aligned with a purely translational movement in map space. This is likely correct: the ~15 m nominal uncertainty in the NAC orbits **[3]** should preclude any major differences in offset from one end of an image to the other, and, by using only near-nadir observations, we can avoid most distortion from incorrect alignment to the LOLA shapemodel during map-projection.

Absolute control: We are currently limited to a single absolute control point to accurately tie the NAC image data to the LOLA topologic reference frame. We attempted to control NAC images to shaded relief images with matching lighting generated from the most recent high-resolution, low-noise LOLA DTMs **[1]**, a method allowing control points at numerous locations. Unfortunately, the uncertainty in that alignment was ~15-20 m due to insufficient detail on the edges of craters in the LOLA DTMs, and small (<~50 m diameter) craters frequently absent. We were, however, able to tie an initial reference image (M121951177R) to the orthophoto of a recently-completed NAC DTM (SHACKRDGE02) to within ~1 m. The DTM, in turn, is tied to LOLA elevation tracks to within ~3.3 m **[4]**, giving an absolute accuracy for that image better than 5 m. This is the only well-aligned NAC DTM in this region.

Method: The central method of this control process is co-aligning a set of map-projected 600x600 m square segments of all images of some arbitrary point across all available lighting conditions.

Starting from a segment of an already-aligned reference image of the point, we sort the segments into a "chain," ordered by sub-solar-longitude relative to the reference image. Then, going segment-by-segment in that order, we attempt to align each to the previous one in the chain that successfully aligned (falling back on earlier segments if needed). After aligning the images in both ascending and descending sub-solar longitude order, the image-to-image offsets are tallied up to produce a net offset from the reference segment (see **Figure 1**). We used the ISIS *findfeatures* tool for alignment **[2,5]**,

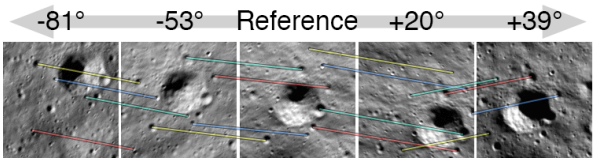

Figure 1: Example chain of images, working out from center. Colored lines mark hypothetical feature matches, which may not use the same features between image pairs. Numbers at top are sub-solar longitude relative to center image (actual image-to-image lighting changes would be much less extreme).

with the SIFT feature detector and matcher algorithm.

We found that for south polar images, where there is usually very dense coverage in terms of solar azimuth and incidence angles. This method tends to align all segments to within about two pixels (2 m) of each other, with the largest offsets found between segments at opposite ends of the chain of alignment.

Occasionally, when an image with a pixel scale larger than the 1 m/px map scale occurs at a large gap in sub-solar longitudes, the segment-to-segment alignment will be incorrect, shifting by up to roughly the lower-resolution image's pixel scale, and making all subsequent offsets in that chain incorrect. We cannot identify this type of error automatically, but mitigate it by excluding images with native pixel scales >3 m/px, and manual inspection of a random sample indicates that ~2% of chains are affected, with errors ≤3 m.

Broader Algorithm: To apply this technique toward creating a large control network, we adopted an iterative approach, building out from image M121951177R. For a given already-aligned reference image, the process splits the image into square segments (usually 22 2500x2500 px segments), map-projects them at 1 m/px, offsets them by the previously-calculated absolute offset, and runs the alignment algorithm above for all images that cover the center point of the segment. This results in newly-calculated absolute cartographic locations for all images that overlapped the reference image.

Upon completing one reference image, the system randomly selects a new reference image that has aligned in at least five chains, prioritizing those that maximized the area not already covered by reference images. We also manually selected some reference images to expand the network into poorly-covered regions.

This process produces two sets of image offsets: One is the absolute position of each NAC image, potentially distorted by accumulation of errors, and one is relative offsets between pairs of NACs, with <~5 m error.

Results: We currently have 637 reference images, 5,875 alignment chains, 39,948 images aligned (of ~50,000 below 85° S), and ~318,000 relative offsets between images. Preliminary mosaics of images near the pole have image-to-image seams <10 m, an improvement over the offsets up to ~100 m that uncontrolled images had in that region. Note, prior uncontrolled mosaics from single weeks of sequential orbits can have ~1 m seams, but rarely align with images with other lighting.

This process's "absolute image position" output was significantly worse than an uncontrolled mosaic. Images at the outer edges of the network shifted hundreds of meters, far more than the relative shifts we see between images. Images were generally shifted towards the pole in Y (near-far axis) and away from the pole in X (leading-trailing axis), proportionally to the distance from the pole. This pattern suggests that there may be an effect beyond the propagation of random errors, although we are still investigating possible causes.

We believe the relative image-to-image offsets will be largely unaffected by whatever is affecting the absolute offsets. The 99th percentile of relative offsets is ~100 m total lateral offset, increasing slightly with latitude. This could correspond to any combination of two offsets from truth that add up to 100 m, far lower than the "absolute" offset numbers we derived. The 95th percentile relative offset is 68 m, just slightly larger than expected from **[6]**, which saw 95th percentile relative offsets of ~50 m at more equatorial sites.

Next steps: Our plan going forward is to use the relative image offsets, which should be independent of any propagation of error, to do a network-wide optimization.

Additionally, we will align the majority of the remaining 20% of images below 85°S, and those from 84-85°S, and verify/improve absolute control with yet-to-be-completed additional NAC DTMs within the area of interest. We intend to use the final image offsets to correct the positions of the polar NAC images on QuickMap and improve the existing NAC south pole mosaic. We are considering ways to publish these image locations in a useable manner.

Conclusions: We are making progress towards full cartographic control of all NAC images of the south polar region. The resulting products should be useful for basemaps for future landed and orbital missions, including the upcoming ShadowCam instrument.

We have found the lighting-agnostic alignment algorithm to be applicable outside of the polar regions as well, although it has difficulty at low phase angles.

References: **[1]** Barker et al. (2021) *PSS*, 203. doi:10.1016/j.pss.2020.105119 **[2]** Anderson et al. (2004), 35th LPSC, #2039. **[3]** Mazarico et al. (2011), *J. Geod.*, 86. doi: 10.1007/s00190-011-0509-4 **[4]** Henriksen et al. (2017), *Icarus*, 283. doi:10.1016/j.icarus.2016.05.012 **[5]** Sides et al. (2017), 48th LPSC, #2739 **[6]** Wagner et al. (2017), *Icarus*, 283. 10.1016/j.icarus.2016.05.011